Polarization of Lyman-α emission in proton-hydrogen collisions studied using a semiclassical two-center convergent close-coupling approach

S. K. Avazbaev, A. S. Kadyrov, I. B. Abdurakhmanov, D. V. Fursa, and I. Bray

Phys. Rev. A **93**, 022710 — Published 22 February 2016

DOI: 10.1103/PhysRevA.93.022710

Polarization of Lyman-α emission in proton-hydrogen collisions studied using a semiclassical two-centre convergent close-coupling approach

S. K. Avazbaev, A. S. Kadyrov, I. B. Abdurakhmanov, D. V. Fursa and I. Bray
Department of Physics and Astronomy, Curtin University, GPO Box U1987, Perth, WA 6845, Australia

The semiclassical convergent close-coupling approach to ion-atom collisions has been extended to include electron-transfer channels. The approach has been applied to study the excitation and the electron-capture processes in proton-hydrogen collisions. The integral alignment parameter A_{20} for polarization of Lyman-α emission as well as the cross sections for excitation and electron-capture into the lowest excited states have been calculated in a wide range of the proton impact energies from 1 keV to 1 MeV. The results are in good agreement with experimental measurements.

PACS numbers: 34.10.+x,34.70.+e,34.50.Fa

I. INTRODUCTION

Processes taking place in proton collisions with atomic hydrogen are of fundamental theoretical and practical importance. For theoretical description of these processes at low incident energies various adiabatic, hyperspherical and molecular-orbital close-coupling methods are used (see, e.g. [1, 2] and references therein). At sufficiently high energies the problem can be treated using the continuum distorted-wave [3–6] and other perturbative methods [7]. However, in the intermediate energy range the cross sections for the excitation of the target, electron capture by the projectile and direct ionization are comparable in magnitude. In this region, non-perturbative methods based on the solution of the time-dependent Schrödinger equation (TDSE) within lattice or various close-coupling schemes allow studying these processes simultaneously.

Since the pioneering work of Bates and McCarroll [8] two-centre coupled channel methods have seen significant development. Earlier works [9–13] with a small number of eigenstates were followed by Shakeshaft [14] to include a large basis set of scaled hydrogenic states. The rapid development in the computing technology made it possible to perform large-basis calculations including pseudostates. However, such calculations of Slim and Ermolaev [15] produced oscillatory structures in the excitation cross sections which were not observed experimentally. Kuang and Lin [16] attributed the existence of these oscillations to the simultaneous use of pseudocontinuum states on both centres. Hence, they proposed to use an asymmetric close-coupling scheme, called bound-bound-continuum (BBC), with pseudocontinuum states either on the target (BBC-T) or on the projectile (BBC-P). In their BBC-T calculations excitation cross sections were stable and well-behaved (meaning smooth, without spurious oscillations), but capture cross sections exhibited unphysical oscillations. At the same time, the BBC-P type expansion produced the opposite picture where capture cross sections were stable, while excitation cross sections became unstable and oscillatory.

An extensive study of proton-hydrogen collision processes was performed by Toshima [17–19] using the two-centre close-coupling approach based on the Gaussian-type orbitals. They demonstrated that the spurious oscillations observed in the excitation and capture channels are due to the strong coupling effect between bound and pseudocontinuum states belonging to different centres. As evidence, it was shown that as the density of pseudocontinuum states increased the oscillatory structures became less prominent. In [19] the author investigated in detail the convergence of the ionisation cross section by performing BBC-T and BBC-P calculations and comparing them with the results of symmetric calculations where the pseudocontinuum states were on both centres. For all three types of expansions fairly similar ionisation cross sections were obtained except for the low-energy region.

The most recent investigation of capture, excitation and ionisation in the p-H collision system using atomic-orbital close coupling is due to Winter [20]. This work extended Shakeshaft's Sturmian calculations by including large number of pseudostates. For the ionisation channel, the results of Winter are in agreement with those reported by Toshima [19].

A semiclassical convergent close-coupling (SC-CCC) method has been developed in [21] and applied to antiproton collisions with multielectron targets [22, 23]. The SC-CCC method utilized a large basis of pseudostates for expansion of the electronic part of the scattering wave function. The Hamiltonian for the target is diagonalized using the orthogonal Laguerre basis resulting in negative- and positive-energy pseudostates. The method did not include rearrangement channels.

Kołakowska *et al.* [24, 25] have developed a lattice-based method to solve the Schrödinger equation. They have calculated excitation and charge transfer cross sections for transitions into $\{1s, 2s, 2p, 3s, 3p, 3d\}$ states in collisions of protons with hydrogen in the ground state. The semiclassical time-dependent Schrödinger equation has been solved using the lattice-based finite differences and Fourier collocation methods. The approach has been further developed by Schultz *et al.* [26] and Pindzola *et al.* [27]. Pindzola and Schultz [28] have later reformulated the approach using the cylindrical coordinates. Another method of numerical integration of the

three-dimensional time-dependent Schrödinger equation based on the Fourier collocation method has been developed by Chassid and Horbatsch [29] with emphasis on differential cross sections. Overall the results of the lattice methods have been found to be in good agreement with experimental data.

Another coupled-channel approach to proton-hydrogen collisions has been proposed by Keim *et al.* [30]. The approach known as a basis-generator method (BGM) provides a basis dynamically adapted to the collision process. It has been applied to calculate the excitation and electron-capture cross sections.

All afore-mentioned approaches rely on the semiclassical approximation, where the nuclear motion is assumed to be along a straight-line trajectory with a constant velocity. This allows separation of electron and nuclear dynamics resulting in approximate TDSE for the electronic part of the scattering wave function. There is another class of close-coupling methods that do not use the semiclassical approximation to separate the electron and nuclear dynamics. These methods also can take into account all possible reaction channels in ion-atom collisions. An impact-parameter Faddeev approach (IPFA) to ion-atom collisions based on the three-body Faddeev equations was developed by Avakov *et al.* [31] and applied to calculate different electron-transfer reactions [32, 33]. In IPFA the effective potentials were taken into account only in the lowest-order approximation corresponding to the so-called 'pole'-type Feynman diagram for electron transfer. Although the calculations of the total and partial electron-transfer cross sections showed good agreement with available experimental data, at high energies this approach overestimated the experimental observations. To improve the theory a three-body eikonal approach (TBEA) [34] was developed. The approach takes into account the next-order 'triangle' Feynman diagrams in the effective potentials. The application of TBEA lead to considerable improvement in the description of the total and partial electron-transfer cross sections. Later, Alt *et al.* [35] demonstrated that the three-body Faddeev approach was also capable of providing reliable differential electron-transfer and elastic-scattering cross sections. Somewhat related to these are the approaches based on the Faddeev-Watson series [36, 37]. However, being perturbative in nature the latter do not take into account the coupling between the channels and are only applicable at sufficiently high incident energies.

A fully quantum-mechanical three-dimensional integral-equation approach to ion-atom collisions has been developed in [38, 39]. However, being time-consuming it did not allow large multi-channel calculations. A quantum-mechanical version of the convergent close coupling (QM-CCC) approach has been developed in the impact-parameter representation and applied to antiproton scattering on atomic hydrogen [40, 41] and helium [42]. In contrast to the SC-CCC, the QM-CCC method utilizes a large basis of Laguerre pseudostates for expansion of the total three-body scattering wave function without separation of the electronic and nuclear motions.

Despite the overall success of the theoretical approaches, the results of various calculations for the seemingly simplest proton-hydrogen system differ and there are some discrepancies with experimental observations. For instance, in the case of the ionisation channel, near the ionisation peak the discrepancy between theory [19, 20, 25] and the experiment [43–45] is from 30 to 45%. In addition, almost a factor of two disagreement exists between experimental measurements [46, 47] and theoretical calculations [20, 48] for the Balmer-α emission. Clearly, an independent *ab initio* two-centre approach would be helpful in clarifying the situation for this most fundamental collision system. Recently, a two-centre QM-CCC method has been developed [49] in order to address some of these problems.

The purpose of this paper is to further develop the SC-CCC method [21–23] to include the electron-capture channels. As a first test, the method is applied to calculate the integral alignment parameter A_{20} for the linear polarization of Lyman-α emission produced in proton-hydrogen collisions. The parameter requires calculations of the excitation and electron-capture cross sections to the lowest (n=2) excited states. Such calculations do not need continuum states on both centres. We generate the Laguerre-based pseudostates to represent the bound and continuum states of hydrogen. The full set of the generated pseudostates are used for the target centre. However, in this work for the projectile centre only the negative-energy pseudostates are used. Thus, the scheme we use is somewhat similar to the BBC-T one mentioned above. However, for the projectile we use the full set of generated negative-energy pseudostates rather than a several eigenstates. This allows one to span the entire space of the bound states of the atom formed by the projectile after capturing the electron. The ionisation cross section, on the other hand, would require the fully symmetric calculations with the complete set of pseudostates on both centres [49].

The experimentally observable degree of linear polarization of Lyman-α emission induced by proton impact on atomic hydrogen and associated integral alignment parameter provide detailed information about the relative population of different magnetic sublevels and can serve as a sensitive test for theory. The earliest experimental values for the polarization of Lyman-α radiation in proton-hydrogen collisions were reported by Kaupilla *et al.* [50] and Hippler *et al.* [51] at low energies (below 25 keV). The most recent experiments by Keim *et al.* [30] covered the energy range from 1 keV to 1 MeV. Along with the experimental data, Keim *et al.* [30] presented the results of the calculations based on the two-centre BGM approach mentioned earlier. Agreement between experiment and theory is good over a wide energy range. However, there are some discrepancies at higher energies. Recently, the polarization of Lyman-α and Balmer-α emissions in the proton-hydrogen collisions has been stud-

ied using the first-order Faddeev-Watson method [37]. The authors considered the excitation channels only and made comparisons with the experimental and theoretical data of Keim *et al.* [30]. The agreement with experiment was better at higher energies where the contribution from the electron-capture channels is expected to be small.

II. TWO-CENTRE SEMICLASSICAL CLOSE-COUPLING METHOD

A. Basic equations

Consider scattering of a proton on the hydrogen atom. We assume the target nucleus is located at a fixed origin and the projectile is moving along a classical trajectory $\boldsymbol{R} = \boldsymbol{b} + \boldsymbol{v}t$, where $\boldsymbol{b}$ is the impact parameter and $\boldsymbol{v}$ is the constant velocity, defined so that $\boldsymbol{b}\cdot\boldsymbol{v} = 0$. The non-relativistic semiclassical time-dependent Schrödinger equation for the electronic part of the total scattering wave function is written as

$$H\Psi(t,\boldsymbol{r},\boldsymbol{R}) = i\frac{\partial\Psi(t,\boldsymbol{r},\boldsymbol{R})}{\partial t}, \tag{1}$$

with the Hamiltonian

$$H = -\frac{1}{2}\Delta_r - \frac{1}{r_T} - \frac{1}{r_P} + \frac{1}{R}, \tag{2}$$

where $\boldsymbol{r}$ and $\boldsymbol{r}_T$ ($\boldsymbol{r}_P$) denote the electronic coordinates with respect to the midpoint of the internuclear axis and the target (projectile) nucleus. (Atomic units are used unless otherwise specified.) The scattering wave function is expanded in terms of target $\psi^T_\alpha(\boldsymbol{r}_T)$ and projectile $\psi^P_\beta(\boldsymbol{r}_P)$ pseudostates as

$$\begin{aligned}\Psi(t,\boldsymbol{r},\boldsymbol{R}) = &\sum_{\alpha=1}^{N_\alpha} a_\alpha(t,\boldsymbol{b})\psi^T_\alpha(\boldsymbol{r}_T)\exp\left[-i\epsilon^T_\alpha t\right]\\ &+\sum_{\beta=1}^{N_\beta} b_\beta(t,\boldsymbol{b})\psi^P_\beta(\boldsymbol{r}_P)\exp\left[-i\epsilon^P_\beta t\right]\\ &\times\exp\left[-i\left(\boldsymbol{v}\cdot\boldsymbol{r}_T + v^2t/2\right)\right],\end{aligned} \tag{3}$$

where N_α (N_β) is the number of states in the target (projectile) centre and ϵ^T_α (ϵ^P_β) is the energy of the target (projectile) electronic state α (β). The expansion coefficients $a_\alpha(t,\boldsymbol{b})$ and $b_\beta(t,\boldsymbol{b})$ at $t\to+\infty$ represent the transition amplitudes into the target and projectile states. The extra phase factor in the second term of Eq. (3) results from the Gaililean transformation which takes into account the fact that in the moving system the captured electron acquires a kinetic energy $mv^2/2$ and momentum $m\boldsymbol{v}$ relative to the target [52].

Substituting this representation of the scattering wave function into the semiclassical Schrödinger equation (1) and using the standard projection technique one obtains the following set of the first-order differential equations for the time-dependent coefficients

$$\begin{cases} i\dot a_{\alpha'} + i\sum\limits_{\beta=1}^{N_\beta}\dot b_\beta K^{(PT)}_{\alpha'\beta} = \sum\limits_{\alpha=1}^{N_\alpha} a_\alpha D^{(T)}_{\alpha'\alpha} + \sum\limits_{\beta=1}^{N_\beta} b_\beta Q^{(PT)}_{\alpha'\beta},\\ i\sum\limits_{\alpha=1}^{N_\alpha}\dot a_\alpha K^{(TP)}_{\beta'\alpha} + i\dot b_{\beta'} = \sum\limits_{\alpha=1}^{N_\alpha} a_\alpha Q^{(TP)}_{\beta'\alpha} + \sum\limits_{\beta=1}^{N_\beta} b_\beta D^{(P)}_{\beta'\beta},\\ \alpha' = 1,2,3,\ldots,N_\alpha,\quad \beta' = 1,2,3,\ldots,N_\beta,\end{cases}$$

where $D^{(T)}$ and $D^{(P)}$ are direct-scattering matrix elements, while $K^{(PT)}$, $K^{(TP)}$, $Q^{(PT)}$ and $Q^{(TP)}$ are rearrangement matrix elements [53]. This system of coupled equations can be written in the matrix form as

$$i\begin{pmatrix}\boldsymbol{I} & \boldsymbol{K}^{(PT)}\\ \boldsymbol{K}^{(TP)} & \boldsymbol{I}\end{pmatrix}\begin{pmatrix}\dot{\boldsymbol{a}}\\ \dot{\boldsymbol{b}}\end{pmatrix} = \begin{pmatrix}\boldsymbol{D}^{(T)} & \boldsymbol{Q}^{(PT)}\\ \boldsymbol{Q}^{(TP)} & \boldsymbol{D}^{(P)}\end{pmatrix}\begin{pmatrix}\boldsymbol{a}\\ \boldsymbol{b}\end{pmatrix}, \tag{4}$$

where $\boldsymbol{I}$ is the identity matrix, submatrices $\boldsymbol{K}$, $\boldsymbol{Q}$ and $\boldsymbol{D}$ contain the corresponding direct-scattering and rearrangement matrix elements. This system is solved subject to the initial boundary conditions

$$\begin{aligned} a_\alpha(-\infty,\boldsymbol{b}) =&\delta_{\alpha1}, && \alpha = 1,2,3,\ldots,N_\alpha,\\ b_\beta(-\infty,\boldsymbol{b}) =&0, && \beta = 1,2,3,\ldots,N_\beta.\end{aligned} \tag{5}$$

B. Pseudostates

Projectile or target pseudostates used in the calculations can be written as

$$\psi_{nlm}(\boldsymbol{r}) = \phi_{nl}(r)Y_{lm}(\hat r), \tag{6}$$

where

$$\phi_{nl}(r) = \sum_{k=1}^{N_l} c^l_{nk}\xi_{kl}(r), \tag{7}$$

and the basis functions $\xi_{kl}(r)$ are made of the orthogonal Laguerre functions

$$\xi_{kl}(r) = \sqrt{\frac{\lambda_l(k-1)!}{(2l+1+k)!}}(\lambda_l r)^{l+1}e^{-\lambda_l r/2}L^{2l+2}_{k-1}(\lambda_l r). \tag{8}$$

Here $L^{2l+2}_{k-1}(\lambda_l r)$ are the associated Laguerre polynomials and λ_l are the exponential fall-off parameter. Expansion coefficients c^l_{nk} are found by diagonalising the Hamiltonian of the hydrogen atom. The diagonalisation procedure gives negative- and positive-energy pseudostates. As the number of pseudostates in each target symmetry increases the lowest negative-energy pseudostates converge to the hydrogen eigenstates while the positive energy pseudostates represent an increasingly dense discretization of the continuum.

C. Observables

The partial cross sections for the individual direct-scattering (di) and electron-exchange (ex) transitions from the ground state are given by

$$\sigma_\alpha^{\rm di} = 2\pi \int_0^\infty db\ bP_\alpha^{\rm di}(b), \tag{9}$$

$$\sigma_\beta^{\rm ex} = 2\pi \int_0^\infty db\ bP_\beta^{\rm ex}(b), \tag{10}$$

respectively, where the transition probabilities are

$$P_\alpha^{\rm di}(b) = |a_\alpha(+\infty, \boldsymbol{b}) - \delta_{\alpha 1}|^2, \tag{11}$$

$$P_\beta^{\rm ex}(b) = |b_\beta(+\infty, \boldsymbol{b})|^2. \tag{12}$$

Integral alignment parameter, A_{20}, characterizes the anisotropy of the atomic states and is defined as [30]

$$A_{20} = \frac{\sigma_{2p_1} - \sigma_{2p_0}}{2\sigma_{2p_1} + \sigma_{2p_0}}, \tag{13}$$

where

$$\sigma_{2p_0} = \sigma_{2p_0}^{\rm di} + \sigma_{2p_0}^{\rm ex}, \tag{14}$$

$$\sigma_{2p_1} = \sigma_{2p_1}^{\rm di} + \sigma_{2p_1}^{\rm ex}. \tag{15}$$

Note that here σ_{2p_1} refers to the $m = 1$ sublevel which is identical to the cross section for the $m = -1$ sublevel.

III. TWO-CENTRE SEMICLASSICAL CONVERGENT CLOSE-COUPLING CALCULATIONS

A. Validation of the computer code

The system of the first-order differential equations (4) has been solved within the range $Z \in (-Z_{\rm max}, Z_{\rm max})$, where $Z \equiv vt$, subject to the initial boundary conditions given by (5). To this end we have developed an adaptive solver similar to the method of Hamming [54], where the integration step is automatically adjusted according to a certain error-control criterion.

The calculation of the direct-scattering matrix elements is relatively straightforward. In this work we use the procedure that has previously been developed and used in the antiproton-hydrogen calculations by Abdurakhmanov *et al.* [40]. In contrast, the evaluation of the rearrangement matrix elements is significantly more challenging. For this reason, we have performed a series of tests to validate the numerical methods for the calculation of the exchange matrix elements. These are described below.

Different techniques for calculating the two-centre rearrangement matrix elements have been reported in the literature. For example, Avakov *et al.* [32] studied the electron transfer in proton-hydrogen collisions using true eigenstates. The authors included only the lowest-order Feyman diagram, corresponding to the electron-proton interaction. In order to be able to compare the effective potentials, in our code (written for pseudostates) we constructed a large basis so that the lowest pseudostates practically reproduce the exact hydrogenic eigenstates and then used in the calculations only the lowest pseudostates. For example, with the exponential fall-off parameter λ_l in the Laguerre functions set equal to 1 for all l and the basis size $N_l = 40 - l$, all $n \leq 4$ eigenstates are reproduced very accurately. Therefore, as a first important test we have compared the impact parameter dependence of the electron-capture probability amplitudes for all possible combinations of the transitions involving eigenstates with $n \leq 4$. An excellent agreement with the corresponding results by Avakov *et al.* [32] has been obtained. To further test the accuracy of the individual exchange matrix elements, we have calculated the Born cross sections for all channels in p-H($1s$) collisions, taking into account both the electron-proton and proton-proton interactions and compared with the corresponding results from Belkić [7]. In this case too, excellent agreement has been obtained.

The next step is testing the coupling between direct and rearrangement channels in calculations with limited number of eigenstates. Lovell and McElroy [55] carried out (2+1) and (1+2) coupled calculations with different combinations of $1s$ and $2s$ hygrogenic states used in target and projectile centres. The authors tabulated excitation and electron-capture cross sections for several energies. We have obtained very good agreement with all their tabulated data, except for the cross section for the excitation of the $2s$ state at 12.5 keV energy when the $1s$ and $2s$ states for the projectile and the $1s$ state for the target centre are used. Since we got an excellent agreement for all transitions at the all other reported collision energies, we believe that there must be a misprint in [55] in the aforementioned transition.

Calculations with the lowest five eigenstates ($1s$, $2s$, $2p_0$ and $2p_{\pm 1}$) reported by Cheshire *et al.* [11] and Rapp and Dinwiddie [13] could serve as a stronger test. These papers give excitation and capture cross sections for all channels in a tabulated form. Comparing our calculated cross sections at corresponding incident energies we conclude that our results also agree well with the results by Cheshire *et al.* [11] and Rapp and Dinwiddie [13]. Winter and Lin [12] performed calculations with only $1s$ in the target centre and $1s$, $2s$, $2p_0$ and $2p_{\pm 1}$ states in the projectile centre. They reported the $2s$ and $2p$ capture cross sections at $E = 25$ and 100 keV which we reproduce as well.

Thus the performed tests validate the current implementation of the two-centre semiclassical close-coupling method and the associated computer code. Next we apply the method to perform large-scale pseudostate calculations.

B. The integral alignment parameter A_{20}

First we calculate the integral alignment parameter A_{20} for the linear polarization of Lyman-α emission produced in proton-hydrogen collisions. Since this quantity requires calculations of the excitation and electron-capture cross sections for the transitions into the lowest (n=2) excited states only, in principle, we do not need continuum states on both centres. In our calculations, we first generate the Laguerre-based pseudostates to represent the bound and continuum states of the target and the projectile. However, in the projectile center the positive-energy pseudostates are truncated as their contribution is small. As mentioned earlier, this scheme is somewhat similar to the BBC-T one mentioned in Introduction. The difference is in that we use the full set of negative-energy pseudostates rather than several eigenstates. This allows one to span the entire space of the bound states of the atom formed by the projectile after capturing the electron.

We set the fall-off parameter λ_l equal to 1 for all l. This allows one to reproduce the ground state of hydrogen with the least number of basis states. In turn this ensures the fastest convergence in the close-coupling calculations. For each l from 0 to $l_{\max}$ we set $N_l = N_{\max} - l$. To achieve convergence in the final cross sections, $l_{\max}$ and $N_{\max}$ are systematically increased. Calculations with various bases are labeled as $(N_{l_\alpha}, N'_{l_\beta})$, prime meaning only negative-energy pseudostates are used. For example, the diagonalisation of the hydrogen Hamiltonian with $N_{\max} = 20$ and $l_{\max} = 3$ gives 74 nl-states. In the nlm notation (including all m with $|m| \leq l_{\max}$) this corresponds to 286 states and 46 of them are of negative energy. These calculations are denoted as $(20_3, 20'_3)$. Similarly, the $(21_3, 21'_3)$ calculations include 53 negative-energy pseudostates and 249 positive-energy pseudostates for the target and only 53 negative-energy pseudostates for the projectile.

We have performed a series of calculations in the energy interval between 1 keV and 1 MeV with increasing $l_{\max}$ and $N_{\max}$ with a particular attention to the convergence of the integral alignment parameter A_{20}, characterising the degree of linear polarization of Lyman-α emission in proton-hydrogen collisions. In Table I we give A_{20} at incident energies $E = 1, 10, 100$ and 1000 keV for $N_{\max}$ from 10 to 21 at the fixed value of the angular momentum $l_{\max} = 3$. In Figure 1 we plot the integral alignment as a function of impact energy with respect to increasing $l_{\max}$ at fixed $N_{\max} = 20$. Table I and Figure 1 show that the integral alignment A_{20} is very well converged with the $(20_3, 20'_3)$ basis. These results have been obtained with $Z_{\max} = 200$. Calculations with $Z_{\max} = 250$ have also been carried out to make sure the results do not depend on them. Hereafter the $(20_3, 20'_3)$ result are simply called as SC-CCC.

TABLE I. (Color online) Convergence of integral alignment A_{20} of Lyman-α emission for proton impact on atomic hydrogen with increasing $N_{\max}$ at fixed $l_{\max} = 3$.

Energy (keV)	$N_{\max}$=10	$N_{\max}$=15	$N_{\max}$=17	$N_{\max}$=18	$N_{\max}$=19	$N_{\max}$=20	$N_{\max}$=21
1	20.92	44.32	45.49	42.66	44.33	44.56	44.68
10	18.08	16.93	16.20	16.32	16.33	16.15	16.08
100	-3.729	-3.757	-3.768	-3.759	-3.752	-3.751	-3.752
1000	16.16	16.19	16.20	16.25	16.24	16.26	16.26

In Figure 2 we plot the calculated integral alignment A_{20} of Lyman-α emission in p+H collisions as a function of the impact energy. The results of different close-coupling calculations are given by curves, while symbols with error bars represent the experimental data. Comparing our results with the experimental data of Hippler *et al.* [51] in the energy range from 1 to13 keV, we observe fairly good agreement. Within 13-25 keV, where there is some disagreement between the experimental measurements of Keim *et al.* [30] and Hippler *et al.* [51] our results are in good agreement with the former. But at higher energies (E >30 keV) our results underestimate the experimental observations of Keim *et al.* [30]. From the theoretical side, comparison is made with the calculations of McLaughlin *et al.* [48], Winter [20] and Keim *et al.* [30]. At lower energies, A_{20} from the 40-state triple centre close-coupling calculations of McLaughlin *et al.* [48] is higher than the results of the current work and the other calculations. The 40-state coupled-channel calculation [48] produces A_{20} that passes through zero at much lower energy than the experiment and the other theories. Similarly, the minimum of A_{20} is reached at much lower energy by the three-centre work [48]. The recent semiclassical 220-Sturmian function results of Winter [20] in the interval between 1 keV and 100 keV show significantly different energy dependence exhibiting double minima at about 20 keV and 50 keV. Reasonably good agreement is achieved with the two-centre BGM calculations of Keim *et al.* [30] over the whole energy range of interest. Especially, the agreement is rather good be-

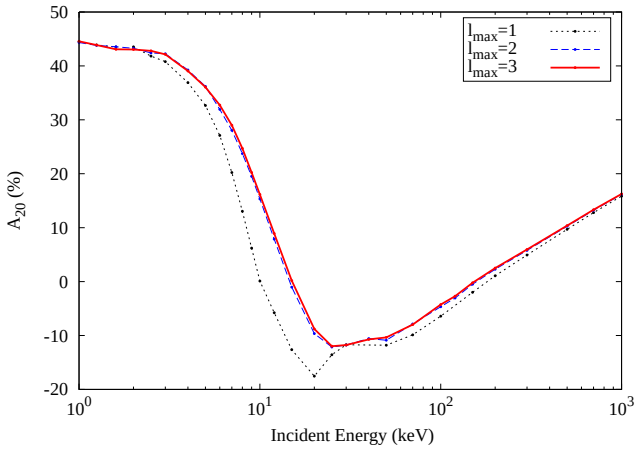

FIG. 1. (Color online) Convergence of integral alignment A_{20} of Lyman-α emission in p+H collisions with respect to increasing $l_{\max}$ at fixed $n_{\max}$=20.

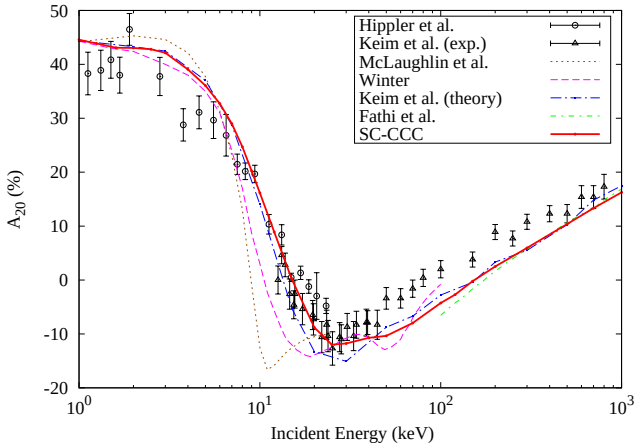

FIG. 2. (Color online) Integral alignment A_{20} of Lyman-α emission in p+H collisions as a function of the impact energy. Experimental results of Hippler *et al.* [51] and Keim *et al.* [30] and theoretical calculations of McLaughlin *et al.* [48], Winter [20], Keim *et al.* [30] and Fathi *et al.* [37] are also given. The results of the present work are given by a red solid line connecting the calculated points.

low 10 keV. In Figure 2, the results of Fathi *et al.* [37] from the three-body Born-Faddeev calculations are also shown. As mentioned before these calculations do not take into account electron capture. The results are close to the ones from the close-coupling techniques above 200 keV which indicate that at high energies the contribution from the electron-capture channels is small.

As seen from Figure 2, A_{20} from the current calculations reproduces the experimental data reasonably well at all considered energies. At low energies, the integral alignment is positive meaning that the cross section for the transition to the $2p_1$ state is much larger than the one corresponding to the $2p_0$ level. As the incident energy increases the cross section for the $2p_0$ channel gets larger resulting in the change of sign at about 15 keV. Here the electron-capture channels become negligible and the excitation channels give the main contribution to the integral alignment parameter. It is interesting to note that, although the integrated cross sections for both the excitation and the electron-transfer channels calculated by the large-scale coupled-channel approaches agree reasonably well with the experiments, the agreement for the relative ratio of cross sections for $2p$ channels (as defined by A_{20}) is not satisfactory at higher energies.

Finally, we emphasise that all previous calculations (except perturbative ones) exhibit oscillations and wiggles (see Figure 2). The latter may indicate that convergence has not been reached in terms of the range of included impact parameters. According to our calculations the probabilities for the $2p_0$ and $2p_1$ transitions have extremely long tails. In fact, the higher the energy, the longer is the tail. For this reason, in order to get convergent (and, therefore, smooth) results we had to include impact parameters as large as 50 a.u.. Test calculations at 1 MeV with the maximum impact parameter 60 and 70 a.u. gave the same result. At the same time, trial calculations with the maximum impact parameter 30 a.u. showed wiggles similar to those seen in A_{20} calculated using the BGM method [30]. The oscillations similar to those seen in the Sturmian-based close coupling method may indicate that the exchange matrix elements, calculated as two-dimensional integrals with the reported integration parameters [20], were not sufficiently accurate. Generally, we find that A_{20} is more demanding in terms of various integration parameters than the individual partial cross sections used to calculate it.

C. Excitation and electron capture into $2s$ and $2p$ states

In Figures 3-6 we present our $2s$ and $2p$ excitation and electron-capture cross sections and compare with experimental measurements and various calculations. The agreement with the calculations of Winter [20] is generally good. However, detailed comparison with Winter's 220-state Sturmian function calculations (see Table V in [20]) reveals that there are some discrepancies. These are clearly noticeable, e.g., at energies 8 and 25 keV. In the $2s$ excitation cross sections (Figure 3), the disagreement at these energies are about 13% and 16%, respectively. While in the case of excitation to the $2p$ state the discrepancies are 5% and 12%, respectively. Interestingly, our cross sections for electron capture to the $2p$ level agree very well with the corresponding results of Winter [20] at all energies.

Also shown in Figs. 3-6 are the cross sections by Kolakowska *et al.* [24] obtained using the lattice-based Fourier collocation method. Our results agree with them at all energies except at 100 keV for excitation to the $2p$ and at 40 keV for electron capture to the $2s$ state. Relatively worse agreement is observed with the calcu-

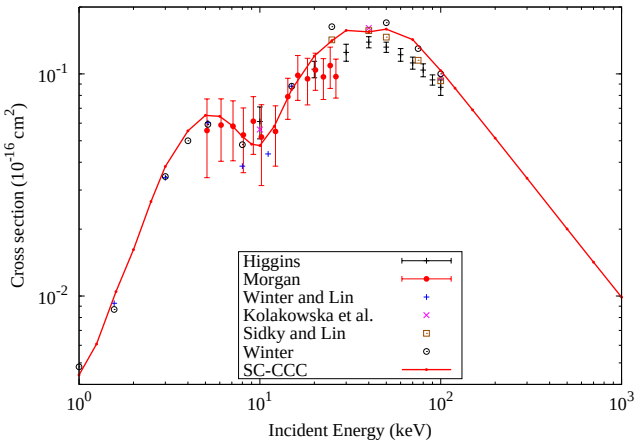

FIG. 3. (Color online) The cross section for excitation to the $2s$ state for the p-H($1s$) collisions. Experimental results of Higgins *et al.* [56] and Morgan *et al.* [57] as well as the theoretical calculations by Winter and Lin [58], Kolakowska *et al.* [24], Sidky and Lin [59] and Winter [20] are shown. The present SC-CCC results are shown by a red solid line. Experimental results are given with error bars, while symbols indicate the theoretical calculations.

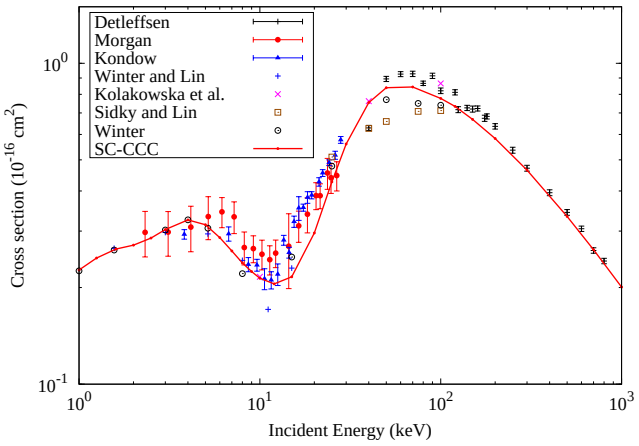

FIG. 4. (Color online) The cross section for excitation to the $2p$ state for the p-H($1s$) collisions. Experimental results are due to Detleffsen *et al.* [60], Morgan *et al.* [57] and Kondow *et al.* [61]. Theoretical calculations are as described in Figure 3.

lations from the two-centre momentum-space discretization method of Sidky and Lin [59]. Significant differences in $2p$ excitation and $2s$ capture cross sections are visible almost at all five energies given by Sidky and Lin [59]. Winter and Lin [58] reported 36-state triple-centre results at E=8, 11.11 and 15 keV. These are also displayed in Figures 3-6. Overall agreement between our results and the calculations of Winter and Lin [58] is not very good. For example, for the $2s$ excitation (Figure 3) at 8 keV the discrepancy is almost 40%. This gets even worse for the $2p$ excitation cross section at E=11.11 keV.

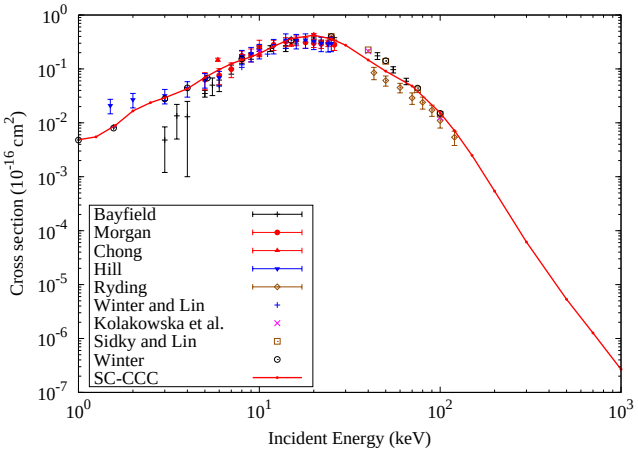

FIG. 5. (Color online) The cross section for electron transfer to the $2s$ state for the p-H($1s$) collisions. Experimental results are due to Bayfield *et al.* [62], Chong *et al.* [63], Hill *et al.* [64], Morgan *et al.* [57] and Ryding *et al.* [65]. Theoretical calculations are as described in Figure 3.

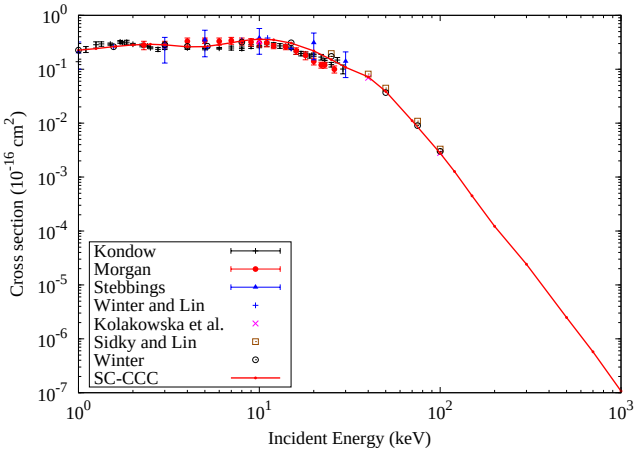

FIG. 6. (Color online) The cross section for electron transfer to the $2p$ state for the p-H($1s$) collisions. Experimental results are due to Kondow *et al.* [61], Morgan *et al.* [57] and Stebbings *et al.* [66]. Theoretical calculations are as described in Figure 3.

For the $2s$ excitation (Figure 3), in the range 5-15 keV there is an excellent agreement with the experimental values of Morgan *et al.* [57]. But at higher energies our results lie slightly above the experimental data of Higgins *et al.* [56]. As it is seen from Figure 4, the $2p$ excitation cross section is in good agreement with the experiment except for the region 15-25 keV. At higher energies our cross sections are within the error bars of the measurements by Detleffsen *et al.* [60]. As to electron transfer to the $2s$ state (Figure 5), our cross sections are in agreement with the experimental data of Bayfield *et al.* [62], Chong *et al.* [63], Hill *et al.* [64] and Morgan *et al.* [57]. But in the 40-100 keV energy interval our results are located between the values given by Bayfield *et al.* [62]

and Ryding *et al.* [65]. Comparison of the calculated $2p$ electron-transfer cross section in Figure 6 shows excellent agreement with the experiment of Kondow *et al.* [61], Morgan *et al.* [57] and Stebbings *et al.* [66].

IV. CONCLUSION

The semiclassical convergent close-coupling approach to ion-atom collisions has been extended to include rearrangement channels. The approach has been applied to calculate the integral alignment parameter A_{20} associated with the degree of linear polarization of Lyman-α emission induced by proton impact on atomic hydrogen over the broad energy range spanning 1 to 1000 keV. It provides detailed information about the relative population of different magnetic substates and can serve a sensitive test for theory. The calculated linear polarisation parameter A_{20} includes contributions to Lyman-α radiation from both direct and exchange excitation of atomic hydrogen and is in good agreement with the most recent measurements of Keim *et al.* [30] as well as earlier experimental data of Hippler *et al.* [51]. However, at higher energies the agreement with the experiments is less satisfactory. Fairly good agreement with the two-centre BGM calculations by Keim *et al.* [30] is obtained. The excitation as well as capture cross sections to the lowest levels of the atomic hydrogen are in excellent agreement with the experimental data.

As mentioned earlier, almost a factor of two disagreement still exists between experimental measurements [46, 47] and theoretical calculations [20, 48] for the Balmer-α emission. Another challenge is calculation of stopping power. The first coupled-channel calculation of the energy loss for protons colliding with H atoms were reported by Grande and Schiwietz [67]. Since then the problem has not been fully resolved. Recently we have reported stopping power calculations for antiprotons in atomic [68] and molecular targets [69]. However, a full solution to the proton-H energy loss problem is more challenging as it requires solution to concurrent H-H problem as well. Grande and Schiwietz [67] considered the latter in the so-called first-order plane-wave Born approximation. It would be interesting to apply the present method to the Balmer-α emission problem and calculations of stopping cross sections for protons colliding with atomic hydrogen.

ACKNOWLEDGMENTS

The work was supported by the Australian Research Council. We are grateful for access to the Australian National Computing Infrastructure Facility and the Pawsey Supercomputing Centre in Western Australia. A.S.K. acknowledges a partial support from the U.S. National Science Foundation under Award No. PHY-1415656. We thank Tom Kirchner for sending data in a tabulated form.

[1] A. Igarashi and C. D. Lin, Phys. Rev. Lett. **83**, 4041 (1999).
[2] S. Zou, L. Pichl, M. Kimura, and T. Kato, Phys. Rev. A **66**, 042707 (2002).
[3] D. Belkic, R. Gayet, and A. Salin, Phys. Rep. **56**, 279 (1979).
[4] A. B. Voitkiv and J. Ullrich, Phys. Rev. A **67**, 062703 (2003).
[5] A. B. Voitkiv, B. Najjari, and J. Ullrich, J. Phys. B **36**, 2591 (2003).
[6] F. D. Colavecchia, G. Gasaneo, and C. R. Garibotti, Journal of Physics B: Atomic, Molecular and Optical Physics **33**, L467 (2000).
[7] D. Belkić, S. Saini, and H. S. Taylor, Phys. Rev. A **36**, 1601 (1987).
[8] D. R. Bates and R. McCarroll, Proceedings of the Royal Society of London A: Mathematical, Physical and Engineering Sciences **245**, 175 (1958).
[9] L. Wilets and D. F. Gallaher, Phys. Rev. **147**, 13 (1966).
[10] D. F. Gallaher and L. Wilets, Phys. Rev. **169**, 139 (1968).
[11] I. M. Cheshire, D. F. Gallaher, and A. J. Taylor, Journal of Physics B: Atomic and Molecular Physics **3**, 813 (1970).
[12] T. G. Winter and C. C. Lin, Phys. Rev. A **10**, 2141 (1974).
[13] D. Rapp and D. Dinwiddie, The Journal of Chemical Physics **57**, 4919 (1972).
[14] R. Shakeshaft, Phys. Rev. A **18**, 1930 (1978).
[15] H. A. Slim and A. M. Ermolaev, Journal of Physics B: Atomic, Molecular and Optical Physics **27**, L203 (1994).
[16] J. Kuang and C. D. Lin, J. Phys. B **29**, 1207 (1996).
[17] N. Toshima, J. Phys. B **25**, L635 (1992).
[18] N. Toshima, J. Phys. B **30**, L131 (1997).
[19] N. Toshima, Phys. Rev. A **59**, 1981 (1999).
[20] T. G. Winter, Phys. Rev. A **80**, 032701 (2009).
[21] I. B. Abdurakhmanov, A. S. Kadyrov, D. V. Fursa, and I. Bray, Phys. Rev. Lett. **111**, 173201 (2013).
[22] I. B. Abdurakhmanov, A. S. Kadyrov, D. V. Fursa, S. K. Avazbaev, and I. Bray, Phys. Rev. A **89**, 042706 (2014).
[23] I. B. Abdurakhmanov, A. S. Kadyrov, D. V. Fursa, S. K. Avazbaev, J. J. Bailey, and I. Bray, Phys. Rev. A **91**, 022712 (2015).
[24] A. Kołakowska, M. S. Pindzola, F. Robicheaux, D. R. Schultz, and J. C. Wells, Phys. Rev. A **58**, 2872 (1998).
[25] A. Kołakowska, M. S. Pindzola, and D. R. Schultz, Phys. Rev. A **59**, 3588 (1999).
[26] D. R. Schultz, M. R. Strayer, and J. C. Wells, Phys. Rev. Lett. **82**, 3976 (1999).
[27] M. S. Pindzola, T. G. Lee, T. Minami, and D. R. Schultz, Phys. Rev. A **72**, 062703 (2005).
[28] M. S. Pindzola and D. R. Schultz, Phys. Rev. A **77**, 014701 (2008).
[29] M. Chassid and M. Horbatsch, Phys. Rev. A **66**, 012714 (2002).
[30] M. Keim, A. Werner, D. Hasselkamp, K.-H. Schartner, H. J. Ldde, A. Achenbach, and T. Kirchner, J. Phys. B

38, 4045 (2005).
[31] G. V. Avakov, A. R. Ashurov, L. D. Blokhinstev, A. M. Mukhamedzhanov, and M. V. Poletayeva, J. Phys. B **23**, 2309S (1990).
[32] G. V. Avakov, A. R. Ashurov, L. D. Blokhintsev, A. S. Kadyrov, A. M. Mukhamedzhanov, and M. V. Poletayeva, J. Phys. B **23**, 4151 (1990).
[33] G. V. Avakov, L. D. Blokhintsev, A. S. Kadyrov, and A. M. Mukhamedzhanov, J. Phys. B **25**, 213 (1992).
[34] E. O. Alt, G. V. Avakov, L. D. Blokhintsev, A. S. Kadyrov, and A. M. Mukhamedzhanov, J. Phys. B **27**, 4653 (1994).
[35] E. O. Alt, A. S. Kadyrov, and A. M. Mukhamedzhanov, Phys. Rev. A **60**, 314 (1999).
[36] S. Alston, Phys. Rev. A **42**, 331 (1990).
[37] R. Fathi, M. A. Bolorizadeh, F. S. Akbarabadi, and M. J. Brunger, J. Phys. B **45**, 205201 (2012).
[38] A. S. Kadyrov, I. Bray, and A. T. Stelbovics, Phys. Rev. A **73**, 012710 (2006).
[39] A. S. Kadyrov, I. B. Abdurakhmanov, I. Bray, and A. T. Stelbovics, Phys. Rev. A **80**, 022704 (2009).
[40] I. B. Abdurakhmanov, A. S. Kadyrov, I. Bray, and A. T. Stelbovics, J. Phys. B **44**, 075204 (2011).
[41] I. B. Abdurakhmanov, A. S. Kadyrov, I. Bray, and A. T. Stelbovics, J. Phys. B **44**, 165203 (2011).
[42] I. B. Abdurakhmanov, A. S. Kadyrov, D. V. Fursa, I. Bray, and A. T. Stelbovics, Phys. Rev. A **84**, 062708 (2011).
[43] M. B. Shah and H. B. Gilbody, J. Phys. B **14**, 2361 (1981).
[44] M. B. Shah, D. S. Elliott, and H. B. Gilbody, J. Phys. B **20**, 2481 (1987).
[45] G. W. Kerby, M. W. Gealy, Y.-Y. Hsu, M. E. Rudd, D. R. Schultz, and C. O. Reinhold, Phys. Rev. A **51**, 2256 (1995).
[46] A. Donnelly, J. Geddes, and H. B. Gilbody, J. Phys. B **24**, 165 (1991).
[47] A. Werner and K.-H. Schartner, Journal of Physics B: Atomic, Molecular and Optical Physics **29**, 125 (1996).
[48] B. M. McLaughlin, T. G. Winter, and J. F. McCann, J. Phys. B **30**, 1043 (1997).
[49] I. B. Abdurakhmanov, A. S. Kadyrov, and I. Bray, J. Phys. B **49**, 03LT01 (2016).
[50] W. E. Kauppila, P. J. O. Teubner, W. L. Fite, and R. J. Girnius, Phys. Rev. A **2**, 1759 (1970).
[51] R. Hippler, H. Madeheim, W. Harbich, H. Kleinpoppen, and H. O. Lutz, Phys. Rev. A **38**, 1662 (1988).
[52] D. R. Bates, Proc. Roy. Soc. A **247**, 294 (1958).
[53] S. Avazbaev, Ph.D. thesis, Curtin University, Perth, Australia (2015).
[54] A. Ralston, *Mathematical methods for digital computers* (New York: John Wiley and Sons, 1960).
[55] S. E. Lovell and M. B. McElroy, Proc. R. Soc. A **283**, pp. 100 (1965).
[56] D. P. Higgins, J. Geddes, and H. B. Gilbody, J. Phys. B **29**, 1219 (1996).
[57] T. J. Morgan, J. Geddes, and H. B. Gilbody, J. Phys. B **6**, 2118 (1973).
[58] T. G. Winter and C. D. Lin, Phys. Rev. A **29**, 567 (1984).
[59] E. Y. Sidky and C. D. Lin, Phys. Rev. A **65**, 012711 (2001).
[60] D. Detleffsen, M. Anton, A. Werner, and K. H. Schartner, Journal of Physics B: Atomic, Molecular and Optical Physics **27**, 4195 (1994).
[61] T. Kondow, R. J. Girnius, Y. P. Chong, and W. L. Fite, Phys. Rev. A **10**, 1167 (1974).
[62] J. E. Bayfield, Phys. Rev. **185**, 105 (1969).
[63] Y. P. Chong and W. L. Fite, Phys. Rev. A **16**, 933 (1977).
[64] J. Hill, J. Geddes, and H. B. Gilbody, J. Phys. B **12**, L341 (1979).
[65] G. Ryding, A. B. Wittkower, and H. B. Gilbody, Proc. Phys. Soc. (London) **89**, 547 (1966).
[66] R. F. Stebbings, R. A. Young, C. L. Oxley, and H. Ehrhardt, Phys. Rev. **138**, A1312 (1965).
[67] P. L. Grande and G. Schiwietz, Phys. Rev. A **44**, 2984 (1991).
[68] J. J. Bailey, A. S. Kadyrov, I. B. Abdurakhmanov, D. V. Fursa, and I. Bray, Phys. Rev. A **92**, 022707 (2015).
[69] J. J. Bailey, A. S. Kadyrov, I. B. Abdurakhmanov, D. V. Fursa, and I. Bray, Phys. Rev. A **92**, 052711 (2015).